RESEARCH ARTICLE

Biomimetic three-dimensional glioma model printed *in vitro* for the studies of glioma cells and neurons interactions

Luge Bai[1,2], Zhiyan Hao[1,2], Sen Wang[1,2], Jiajia Zhou[1,2], Siqi Yao[1,2], Na Pei[1,2], Hui Zhu[1,2], Kun Zhang[3], Rui L. Reis[4,5], J. Miguel Oliveira[4,5], Jiankang He[1,2], Dichen Li[1,2], Xinggang Mao[6]*, Ling Wang[1,2]*

[1]School of Mechanical Engineering, Xi'an Jiaotong University, Xi'an 710054, Shaanxi, China

[2]NMPA Key Laboratory for Research and Evaluation of Additive Manufacturing Medical Devices, Xi'an Jiaotong University, Xi'an 710054, Shaanxi, China

[3]Department of Pharmacology, School of Pharmacy, Fourth Military Medical University, Xi'an, Shaanxi, China

[4]3B's Research Group, I3Bs – Research Institute on Biomaterials, Biodegradables and Biomimetics, University of Minho, Headquarters of the European Institute of Excellence on Tissue Engineering and Regenerative Medicine, AvePark, Zona Industrial da Gandra, 4805-017 Barco -Guimarães, Portugal

[5]ICVS/3B's - PT Government Associate Laboratory, Braga/Guimarães, Portugal

[6]Department of Neurosurgery, Xijing Hospital, the Fourth Military Medical University, Xi'an, Shaanxi, China

(This article belongs to the *Special Issue: Advances in 3D bioprinting based on lab-on-a-chip platforms for precision oncology*)

*Corresponding authors:
Ling Wang
(menlwang@xjtu.edu.cn)

Xinggang Mao
(xgmao@fmmu.edu.cn)

Abstract

The interactions between glioma cells and neurons are important for glioma progression but are rarely mimicked and recapitulated in *in vitro* three-dimensional (3D) models, which may affect the success rate of relevant drug research and development. In this study, an *in vitro* bioprinted 3D glioma model consisting of an outer hemispherical shell with neurons and an inner hemisphere with glioma cells is proposed to simulate the natural glioma. This model was produced by extrusion-based 3D bioprinting technology. The cells survival rate, morphology, and intercellular Ca^{2+} concentration studies were carried out up to 5 days of culturing. It was found that neurons could promote the proliferation of glioma cells around them, associate the morphological changes of glioma cells to be neuron-like, and increase the expression of intracellular Ca^{2+} of glioma cells. Conversely, the presence of glioma cells could maintain the neuronal survival rate and promote the neurite outgrowth. The results indicated that glioma cells and neurons facilitated each other implying a symbiotic pattern established between two types of cells during the early stage of glioma development, which were seldom found in the present artificial glioma models. The proposed bioprinted glioma model can mimic the natural microenvironment of glioma tissue, provide an in-depth understanding of cell–cell interactions, and enable pathological and pharmacological studies of glioma.

***Keywords**: In vitro* 3D model; Glioma model; 3D bioprinting; Glioma cells; Neurons

1. Introduction

Glioma is the most frequent primary intracranial tumor[1], which accounts for approximately 25.2% of all CNS tumors, and about 82.7% of all malignant tumors[2]. Glioma accounts for 51.3% of tumors in children age 0–14 years[2]. Among children's diseases, glioma is ranked the second in prevalence, just after leukemia[1]. There has also been a significant increase in malignant glioma incidence from 2000 to 2018[2]. Glioma is aggressive with a tendency to recur. Frequently, it is treated by a combination of chemotherapy and pharmacotherapy after surgical resection[2-4]. However, existing drugs have poor effectiveness, with a median survival period of only 12–15 months[5]. Meanwhile, there is a high failure rate of up to 95% in new drug development due to the lack of adequate screening models. Therefore, the biofabrication of mimetic glioma models for the better understanding of the characteristics of the disease, developing antiglioma chemotherapeutic drugs and personalized treatments, and prolonging the life of patients is of great significance.

Currently, the models used for glioma research mainly include animal models and *in vitro* models[6]. Animal models have been established to study glioma progression *in vivo*[7]. However, its applications are limited not only by the interspecies differences between animals and humans, but also by the long-making process, high cost, as well as moral and ethical issues[7]. *In vitro* models sprout to overcome the limitations of animal models. The emphasis of constructing glioma *in vitro* models is to simulate tumor microenvironment (TME), which includes cell–cell and cell–extracellular matrix (ECM) interactions. The *in vitro* two-dimensional (2D) model is most widely used for some basic drug research due to its simplicity. However, with cells cultured in a flat dish, 2D model cannot represent the spatial relationship between the glioma cells and the other species of cells around them in a natural glioma tissue, which plays an important role in TME[8,9]. On the contrary, the 3D models can better represent similar tissue in human, which can provide the 3D space for better cell proliferation and interaction as compared with the 2D model[10]. Glioma stem cells (GSCs), which can self-renew and form 3D spheres known as glioma neurospheres containing multiple cell types in glioma progression[11,12], are used as an important tool for high-throughput drugs screening[13]. However, GSCs cannot retain the ECM to provide the full picture of glioma. Therefore, it is necessary to design and develop novel glioma *in vitro* 3D models to properly reflect the TME similar to that found *in vivo*.

A growing line of evidence corroborates the fact that the complex and dynamic cell–cell interactions can affect the fate of glioma cells and the cells around them, which is a crucial factor for the development of glioma[5]. In the growth environment of glioma tissue, glioma cells communicate with surrounding cells through transmembrane receptors, ligands, and signaling factors, which can regulate tumor progression[14,15]. Several studies have shown that glioma cells tend to grow around neurons[16,17], and neurons can play a crucial role in the occurrence and development of glioma[18]. Using optogenetic method in murine model, Venkatesh *et al.*[18] demonstrated that neurons facilitated the growth of glioma cells by secreting neuroligin-3 and promoted the depolarization and proliferation of glioma cells. Fu *et al.*[19] cultured glioma cells and neurons in the top or bottom chamber, respectively, of 2D trans-well model. It was found that glioma cells exhibited a higher proliferation rate (140%), and the neurons underwent excitotoxicity and damage. These studies indicated that the direct and indirect activities between neurons and glioma cells may be critical factors in regulating glioma progression. Therefore, the study and treatment of glioma disease will significantly advance, if realistic glioma models that replicate the microenvironment to examine the interactions between glioma cells and surrounding neurons become available. Several models[20-22] have been developed to simulate the complex interactions between glioma cells and the surrounding neurons *in vitro* and 3D co-culture model has the greatest potential among them.

Bioprinting is a range of promising technologies to fabricate 3D models of *in vitro* biological tissues due to its excellent ability of fabricating complex structure and dispensing multimaterials. Although the printing resolution of extrusion bioprinting is inferior as compared to other printing techniques, such as droplet-based inkjet printing[23] and laser-induced forward transfer[24], it has been reported to present a decreased damage to cells by adjusting the viscosity of bioink[25]. It is also advantageous as it involves few restrictions on materials, it is convenient and fast to use, and it can better mimic the native tissue microenvironment, so it becomes a common way to fabricate 3D models of *in vitro* biological tissues[26]. As the main component of ECM, collagen has excellent biocompatibility which can support cell growth, migration, and function[27]. Besides, collagen shows high viscosity at low temperature, which makes it one of the most widely materials for bioprinting[28].

In this study, inspired by the microenvironment in which glioma cells are surrounded by neurons, a bioprinted glioma *in vitro* 3D model with glioma cells in the inner layer and with neurons in the outer layer (G/N) was creatively designed and bioprinted to achieve the co-culture of neurons and glioma cells spatially and functionally. For comparison, two additional models were developed, i.e., a 3D model with glioma cells in the inner layer and without

any cells in the outer layer (G) and a 3D model without any cells in the inner layer and with neurons in the outer layer (N). The morphology and number of both types of cells were respectively studied in these three models to analyze the interactions between neurons and glioma cells in *in vitro* glioma tissue. We advance with the novel design and *in vitro* 3D model fabricated by extrusion-based 3D bioprinting to mimic the natural interactions between neurons and glioma cells, which provides a potential way to study the pathological process and treatment of glioma.

2. Materials and methods

2.1. Materials

Sprague Dawley (SD) rats and Kunming mice were provided by the experimental animal center of Fourth Military Medical University (FMMU) (Xi'an, China). GL261 cell lines were purchased from Shanghai Zhongqiao Xinzhou Biotechnology Co., Ltd (Shanghai, China). Trypsin, Dulbecco's modified eagle medium (DMEM), penicillin/streptomycin, and phosphate-buffered solution (PBS) were purchased from Hyclone (South Logan, UT, USA). Fetal bovine serum (FBS), L-glutamine, and B27 neural supplement were purchased from Gibco (Grand Island, NY, USA). Hank's balanced salt solution (HBSS) and LIVE/DEAD Viability/Cytotoxicity Kit were purchased from Thermo Fisher Scientific (Waltham, MA, USA). Fluo-4, AM was purchased from Invitrogen (Camarillo, CA, USA).

2.2. Structure design of the bioprinted glioma *in vitro* 3D model

In clinical cases, glioma cells are found to be wrapped with neurons to form a double-layer spherical glioma tissue (Figure 1A[29]). Bearing such architecture in mind, the design of a novel bioprinted glioma *in vitro* 3D model (G/N) was advanced as depicted in Figure 1B. The simplified bilayer hemispherical model was established as an artificial 3D microenvironment to represent the spherical tissue and replicate the spatial relationship between neurons and glioma cells in actual tissues. In this model, the radius of the inner hemisphere loaded with glioma cells is 4 mm, and the thickness of the outer layer with neurons is 2 mm. To probe the interactions between neurons and glioma cells in the designed model, two controls were set up, which only contains glioma cells in the inner layer (G, Figure 1C) and neurons in the outer layer (N, Figure 1D), respectively.

2.3. Cell culture

Mouse primary cortical neurons were isolated from E14 mouse embryos. The optimized methods were carried out under sterile conditions as fast as possible in order to avoid obtaining damaged neurons. After decapitation, the brain was exposed, the meninges of the cortex region were removed and the cortex tissue was collected and digested with trypsin for 20 min at 37°C. After incubation, the reaction was inhibited by the addition of DMEM containing 10% FBS. The supernatant was discarded by aspiration. The digested tissue was soaked with fresh medium containing DMEM added with 1% L-glutamine, 2% B27 neural supplement, and 1% penicillin/streptomycin. The tissue was mechanically dissociated with a pipette and then filtered through a 40-μm cell strainer. The volume of 20 μL of cell suspension was added to 180 μL of DMEM, and 20 μL of the diluted cell solution was used to perform cell counting by cellometer (Nexcelom Biosciences). Finally, the cell suspension was ready for further bioink preparation.

The GL261 cells, the murine glioblastoma multiforme (GBM) cells, were cultured in DMEM supplemented with 10% FBS and 1% penicillin/streptomycin in advance for a period of 2 days.

2.4. Bioink preparation

The collagen solution (4 mg/mL) was harvested from the tail of SD rats and filter-sterilized prior to use. Collagen solution was mixed with DMEM with a blending ratio of 1:1 (v/v) to prepare collagen solution (2 mg/mL) at 0°C. A 0.5 M NaOH solution was added dropwise in order to adjust the pH value to about 7.4. An appropriate amount of cell suspension was taken according to the amount of bioink and required cell density (neuron: 6×10^6 cells/mL and GL261 cell: 1×10^6 cells/mL). After centrifuging the cell suspension and removing the supernatant, the collagen solution (2 mg/mL, pH 7.4) was added gradually and blown gently in order to obtain the neuron bioink and the GL261 cell bioink (Figure 2A). The prepared bioink was placed at 0°C for bioprinting.

2.5. Bioprinting of the glioma in vitro 3D model

The bioprinting was performed by an in-house developed 3D printer (Figure 2B). Bioinks were loaded in printing barrels in an ice bath and extruded by air pressure. Some main printing parameters are given as follows: needle travel speed of 15 mm/s, air pressure of 320 mbar, needle diameter of 0.2 mm, printing temperature of 0°C, initial layer height of 0.3 mm, and layer height of 0.2 mm. The bioprinting of the glioma 3D model was achieved in a two-step manner as depicted in Figure 2B–G. Firstly, the neuron tissue in the outer layer was formed (a hemispherical shell with 12 mm external diameter and 8 mm internal diameter). Then, the glioma tissues in the inner layer were shaped (a hemisphere with 8 mm diameter). Prior to bioprinting, the equipment was sterilized with overnight exposure to ultraviolet (UV) light. The neuron bioink and the GL261 cell bioink were transferred aseptically into separate printing barrels with attached needles, and then connected to the pneumatic hoses of the 3D printer. The G-code was generated using the printer software and loaded into the 3D
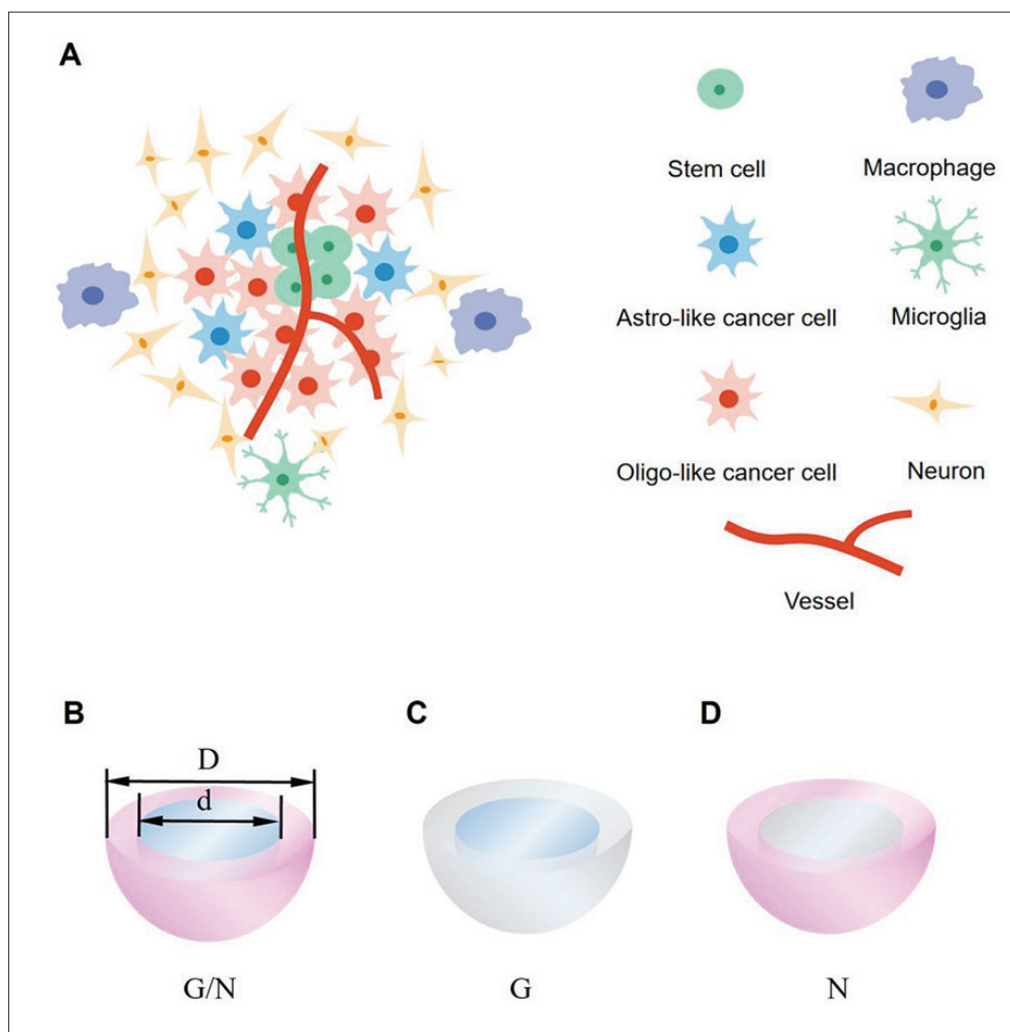
Figure 1. Diagram of glioma microenvironment and the bioprinted 3D models. (A) Diagram of glioma microenvironment, in which glioma cells are wrapped with neurons[29]. (B) The bioprinted glioma *in vitro* 3D model with glioma cells in the inner layer and neurons in the outer layer (G/N) (d = 8 mm, D = 12 mm). (C) The bioprinted 3D model with glioma cells in the inner layer and no cell in the outer layer (i.e., G). (D) The bioprinted 3D model with no cells in the inner layer and neurons in the outer layer (i.e., N). The dimensions of the three models are the same.

printer to form the print paths. After the parameter was set for printing, the bioink was extruded and assembled in a receiving mold. As the forming container for the model, the receiving mold consisted of hemispherical silicone negative mold with a diameter of 12 mm and hemispherical UV-cured positive mold with a diameter of 8 mm to match the fabrication method. After printing neuron bioink into the gap between the positive and negative mold, the resulting external hemispherical shell was completely crosslinked by being incubated at 37°C for 30 min. The preliminary model was taken out of the incubator and gently placed at the center of the printing platform. The positive mold was removed and GL261 cell bioink was printed to shape the internal hemisphere, which was incubated at 37°C for another period of 30 min. The glioma *in vitro* 3D model was formed, and then placed into non–tissue-culture-treated 24-well plates

for culture in the same medium as neurons, which has been proven to be suitable for GL261 cells. The culture medium was changed every 48 h.

In addition, in order to better understand the interactions between neurons and glioma cells in the designed model, two controls were set up, which were G and N conditions. For G control, the bioink used was GL261 cell bioink in the inner layer and collagen (2 mg/mL, pH 7.4) in the outer layer. For N control, the bioink used was collagen (2 mg/mL, pH 7.4) in the inner layer and neuron bioink in the outer layer. The two types of models were fabricated by means of performing the aforementioned biofabrication method.

For better representing the hierarchical structure of the constructed glioma 3D model, Trypan Blue solution
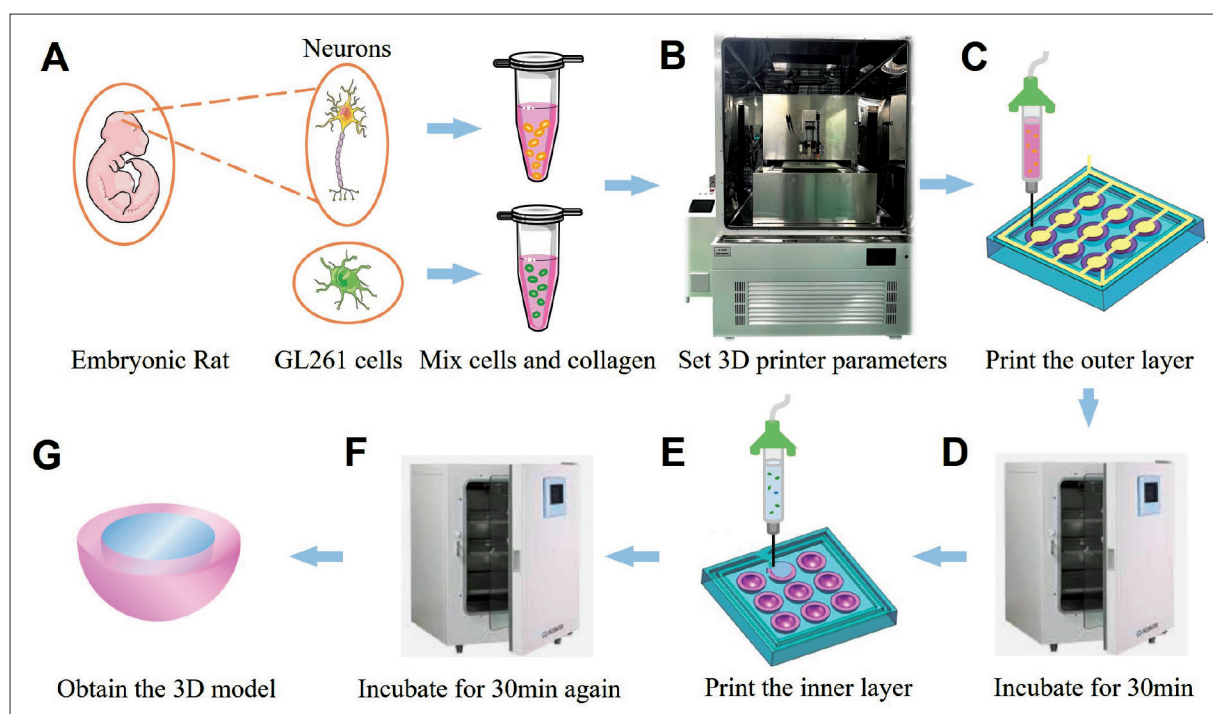
Figure 2. Biofabrication process of the bioprinted glioma *in vitro* 3D model. (A) Neurons from embryonic rat or GL261 cells were respectively mixed with collagen to obtain bioinks. (B) Bioinks were loaded into the barrels of the in-house developed 3D printer, and printing parameters were set. (C) The outer layer of the 3D model was printed. (D) The outer layer of the 3D model was completely crosslinked by being incubated at 37°C for 30 min. (E) The inner layer of the 3D model was printed. (F) The inner layer of the 3D model was completely crosslinked by being incubated at 37°C for 30 min. (G) The bioprinted glioma *in vitro* 3D model was obtained.
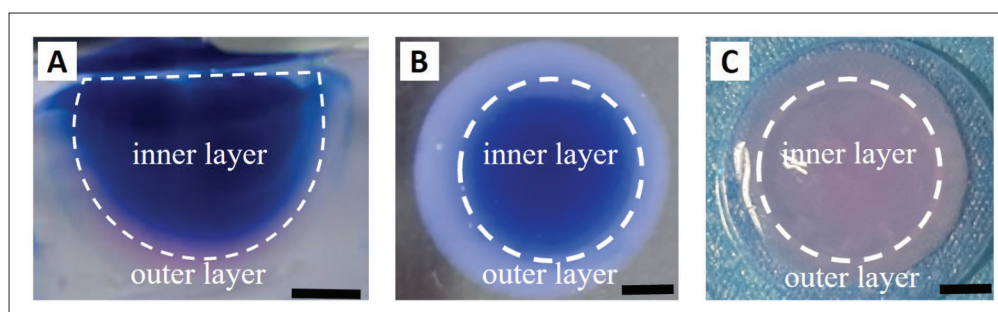
Figure 3. Photographs of the bioprinted glioma *in vitro* 3D model. (A) The main view of the bioprinted glioma *in vitro* 3D model whose inner layer was stained by Trypan Blue. (B) The vertical view of the bioprinted glioma *in vitro* 3D model whose inner layer was stained by Trypan Blue. (C) The vertical view of the bioprinted glioma *in vitro* 3D model with cells. Scale bar = 2 mm.

was added into collagen to print the inner hemisphere, and Trypan Blue-free collagen was used to print the outer hemisphere shell. As shown in Figure 3, the model fabricated by bioprinting method possessed a complete and clear layered structure, which could be used to explore the interactions between neurons and glioma cells *in vitro*.

2.6. Staining and imaging
2.6.1. Cell morphology and distribution
The GL261 cells we purchased were with green fluorescence so that the cell morphology and distribution could be observed directly under a laser scanning confocal microscope (LSCM) (A1, Nikon, Japan). After 5 days of culture, specimens were mounted onto glass slides. Observation and photographing were performed, and each experiment was repeated three times ($n = 3$).

2.6.2. Intracellular Ca2+
After 5 days of culture, specimens were removed from medium and washed three times with HBSS. A 4 μM working solution of fluo-4, AM in PBS was pipetted to cover the specimens. After a 30 min of incubation at 37°C, specimens were washed three times with HBSS followed by another 30-min incubation at 37°C. The fluorescence

image of Ca^{2+} was examined at excitation wavelength of 488 nm under a laser scanning confocal microscope (LSCM) (A1, Nikon, Japan). ImageJ software was used for the quantification of fluorescence intensities. Each experiment was repeated three times ($n = 3$).

2.6.3. Live/dead cell assay

LIVE/DEAD Viability/Cytotoxicity Kit was used to label both live and dead cells in the printed structure. On days 1, 3, and 5 of tissue culture, specimens were harvested from incubator and washed three times in PBS. Later, live/dead working solutions were applied simultaneously to the specimens, and the specimens were then kept in a dark environment. Specimens were washed once before imaged. Exciting light waves were of 515 nm and 580 nm for live and dead cells imaging, respectively. The live cells were in green whilst the dead cells were in red. Z-stacks of 50–90 μm in height were flattened, and the green and red channels were analyzed separately to determine numbers of live and dead cells. Live and dead cells numbers were counted using ImageJ, and the percentage of viable cells was quantified as the number of live cells divided by the total number of cells. Each experiment was repeated three times ($n = 3$).

2.7. Statistical analysis

Statistical analysis was applied to evaluate significant differences among experimental data sets. To obtain statistical results, the number (n) of data sets should be more than 3, or n ≥3. Two-way analysis of variance (ANOVA) was used to investigate the trend of a series of data sets, whereas t-test was used to compare two data sets based on the difference of their characteristics. *p, **p, ***p, and ****p were used to measure the degree of significance: *$p < 0.05$, **$p < 0.01$, ***$p < 0.001$, and ****$p < 0.0001$.

3. Results

3.1. Effects of neurons on GL261 cells in the bioprinted glioma in vitro 3D model

3.1.1. Cell morphology and distribution of GL261 cells

After 5 days of culture, the cell morphology and distribution of GL261 cells in the different *in vitro* 3D models was observed by LSCM (Figure 4A and B). Visual inspection demonstrated that the morphology and distribution of GL261 cells co-cultured with neurons in G/N specimens showed difference in the area far away from neurons and in the area close to neurons. Thus, the observation area in specimens were divided into Far area (the area away from neurons) and Near area (the area near neurons) (Figure 4C). GL261 cell morphology was found diverse, i.e., some cells were spherical, and the other were elongated with filopodium in the Near area in G/N, but

only spherical in the Far area in G/N and in the whole area in G. In order to quantitatively analyze the distribution of GL261 cells in different models, the number of GL261 cells in different areas and models was statistically counted by ImageJ software (Figure 4D). It was found that the amount of GL261 cells in the Near area (42.33 ± 4.72) were significantly higher than those in the Far area (21.33 ± 2.01) in G/N. In addition, the amount of GL261 cells in both the Far and Near area in G/N were superior to that observed in the whole area in G.

3.1.2. Intercellular Ca2+ concentration of GL261 cells

After 5 days of culture, the intracellular Ca^{2+} in the specimens was stained with cell calcium staining agent and imaged by LSCM (Figure 5A and B). The fluorescence intensity of the images was carried out with ImageJ software to analyze the intracellular Ca^{2+} concentration quantitatively (Figure 5C). Similar to cell morphology and distribution, intracellular Ca^{2+} concentration of GL261 cells in G/N also showed differences in the Far and Near areas. Compared with the GL261 cells in the Far area in G/N, those in the Near area in G/N significantly expressed higher fluorescence intensity of Ca^{2+}, which is not found in G. In addition, the intracellular Ca^{2+} concentration in both the Far and Near areas in G/N is higher than that observed in the whole area in G.

3.2. Effects of GL261 cells on neurons in the bioprinted glioma *in vitro* 3D model

3.2.1. Survival rate of neurons

After 1, 3, and 5 days of culture, a live/dead assay was carried out, images of different bioprinted 3D models were obtained by LSCM (Figure 6A). The survival rate of neurons was analyzed quantitatively (Figure 6B). On day 1, it was shown that the neuron survival rate in G/N was 70.24 ± 2.78%, which was 60.00 ± 2.76% in N. After 3 days, the survival rate of neurons in the two models was approximately equal (87.71 ± 1.23% in G/N and 87.36 ± 1.19% in N) and much higher than that observed on day 1. After 5 days of culture, the survival rate of neurons began to decline in both models, which was 58.31 ± 1.09% in G/N and 54.57 ± 1.44% in N. From day 1 to day 5, neurons in G/N consistently exhibited equal or higher survival rates than that observed in N.

3.2.2. Neurite characteristics of neurons

As shown in Figure 6A, a superior proportion of neurons in G/N outgrew neurites and formed connections with each other than those in N after 1 day and 3 days of culture. The neurite characteristics of neurons in the bioprinted 3D models were analyzed using Image J software, and the results obtained are shown in Figure 7. During the 5 days of culturing, the neurite number of individual neurons in both G and N models showed a slight decrease. The neurons in
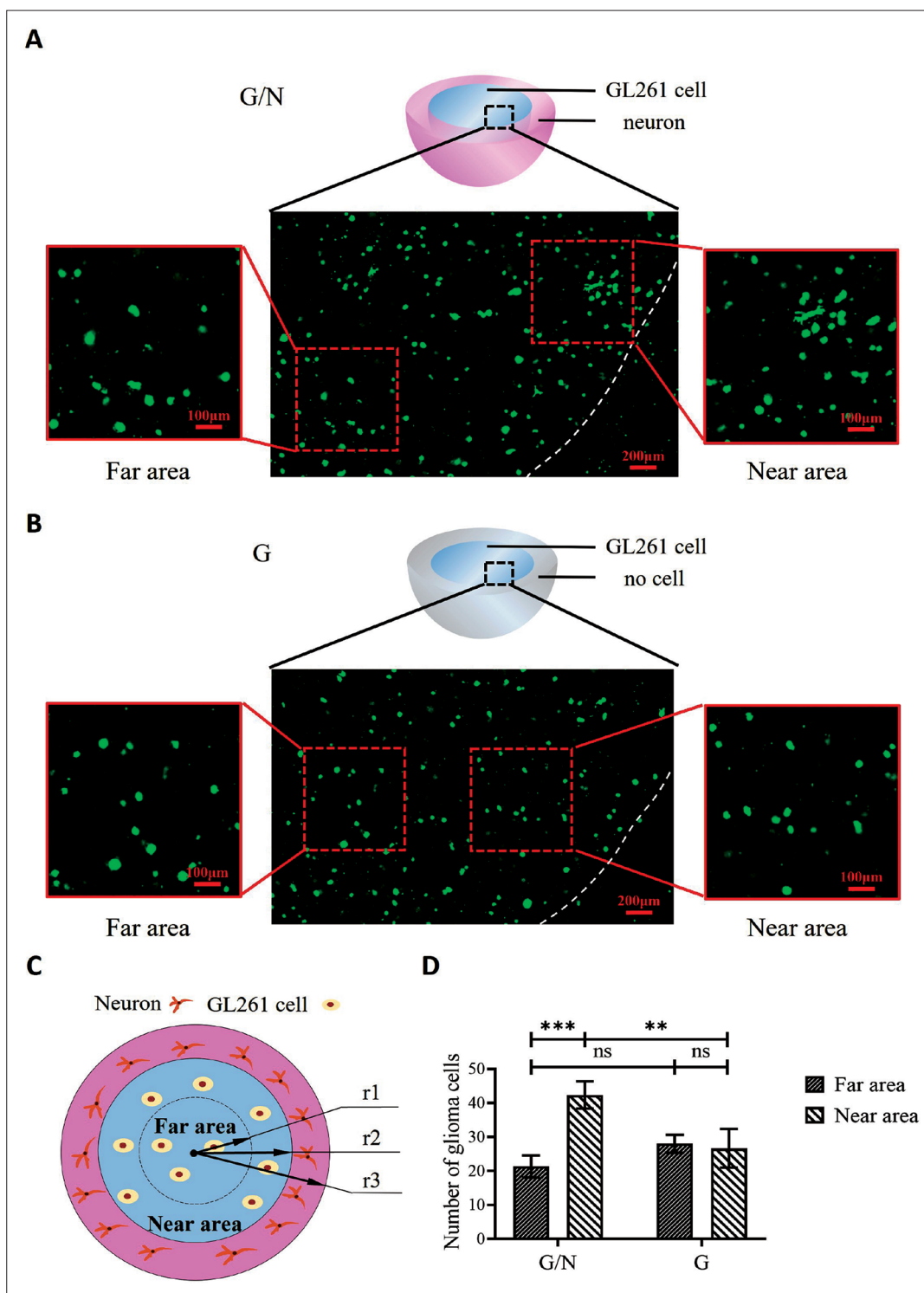
Figure 4. Morphology and distribution of GL261 cells in G/N and G after 5 days of culture. (A) Confocal images of the GL261 cells in the Far area and Near area in G/N. (B) Confocal images of the GL261 cells in the Far area and Near area in G. (C) Diagram of the Near area and the Far area in the observation area of the bioprinted glioma *in vitro* 3D model (r1 = 2 mm, r2 = 4 mm, r3 = 6 mm). (D) Cell number distribution of GL261 cells in G/N and G. Significance was calculated using two-way ANOVA followed by *t*-test. All error bars are standard deviation. $*p < 0.05$, $**p < 0.01$, $***p < 0.001$, and $****p < 0.0001$, respectively.
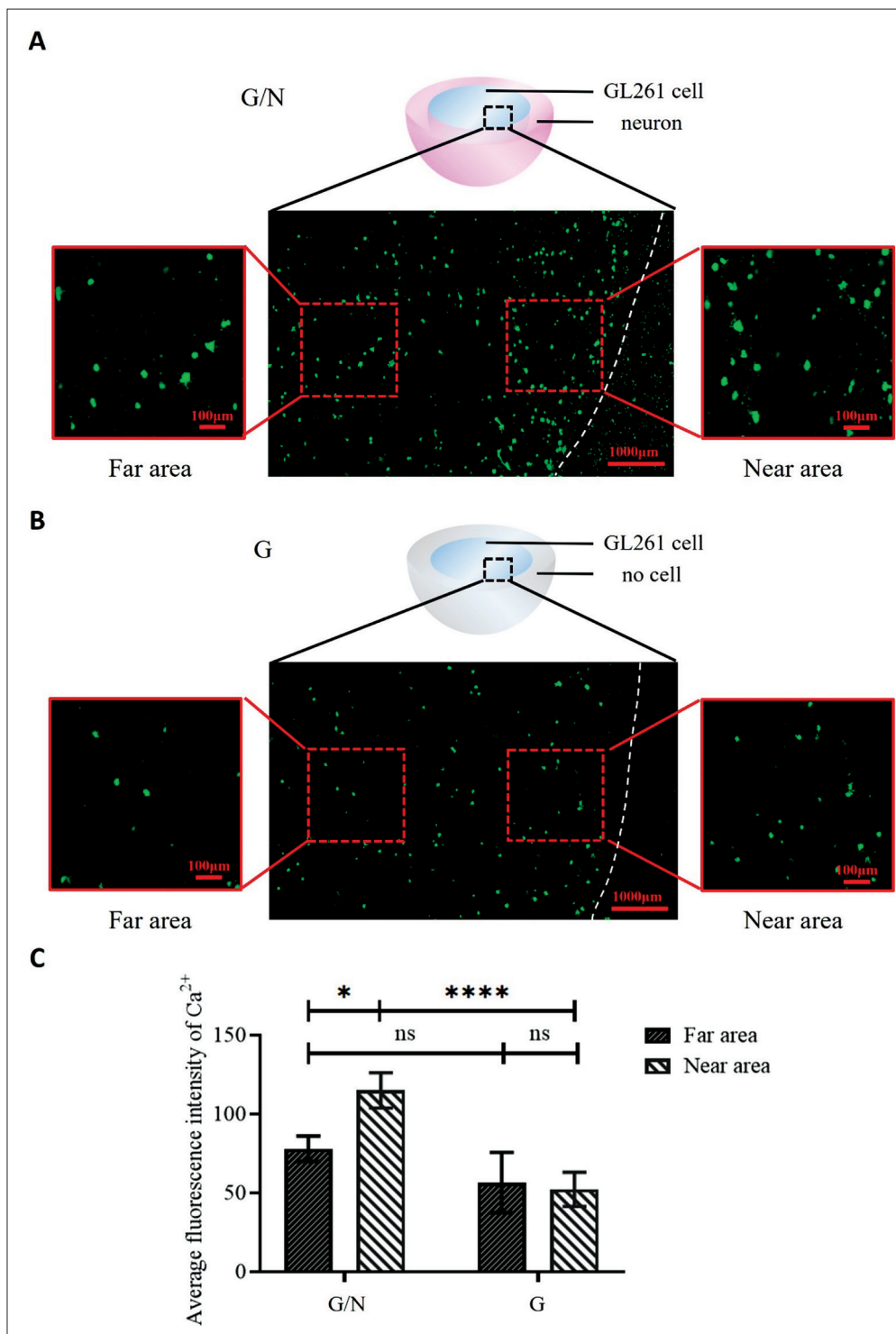
Figure 5. The intracellular Ca²⁺ concentration of GL261 cells in G/N and G after 5 days of culture. (A) The fluorescence confocal image of intracellular Ca²⁺ of the GL261 cells in G/N. (B) The fluorescence confocal image of intracellular Ca²⁺ of the GL261 cells in G. (C) Quantitative analysis of fluorescence intensity of Ca²⁺ of GL261 cells in G/N and G. Significance was calculated using two-way ANOVA followed by t-test. All error bars are standard deviation. $*p < 0.05$, $**p < 0.01$, $***p < 0.001$, and $****p < 0.0001$, respectively.
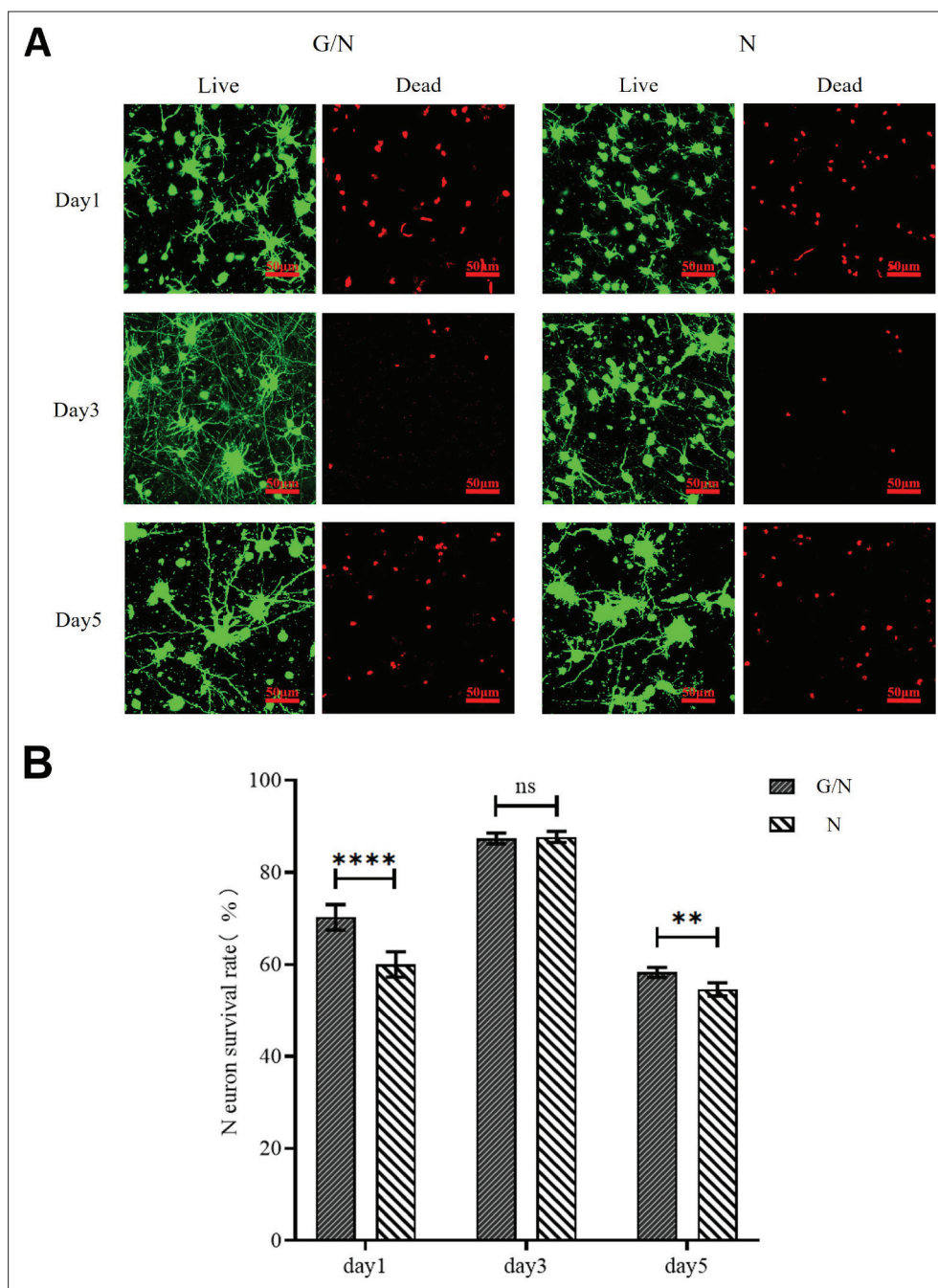
Figure 6. The survival rate of neurons in G/N and N after 1, 3, and 5 days of culture. (A) Confocal images of live/dead staining (green color: live cells; red color: dead cells) of neurons. (B) Histograms of the survival rate of neurons in G/N and N. Significance was calculated using two-way ANOVA followed by t-test. All error bars are standard deviation. $*p < 0.05$, $**p < 0.01$, $***p < 0.001$, and $****p < 0.0001$, respectively.

G/N outgrew significantly more neurites and longer axons in G/N than that found in N during the 5 days of culturing.

4. Discussion

In conventional cell co-culture models, two or more cell types are seeded onto 2D planar cell culture dishes or 3D scaffolds after being mixed evenly, which cannot precisely represent the spatial relationship of different types of cells found *in vivo*[30-32]. In this paper, we propose a novel bilayer glioma 3D *in vitro* model and provide a step-by-step biofabrication method utilizing a removable UV-cured mold to bioprint neurons in the outer layer and glioma cells in the inner layer. Compared with the traditional
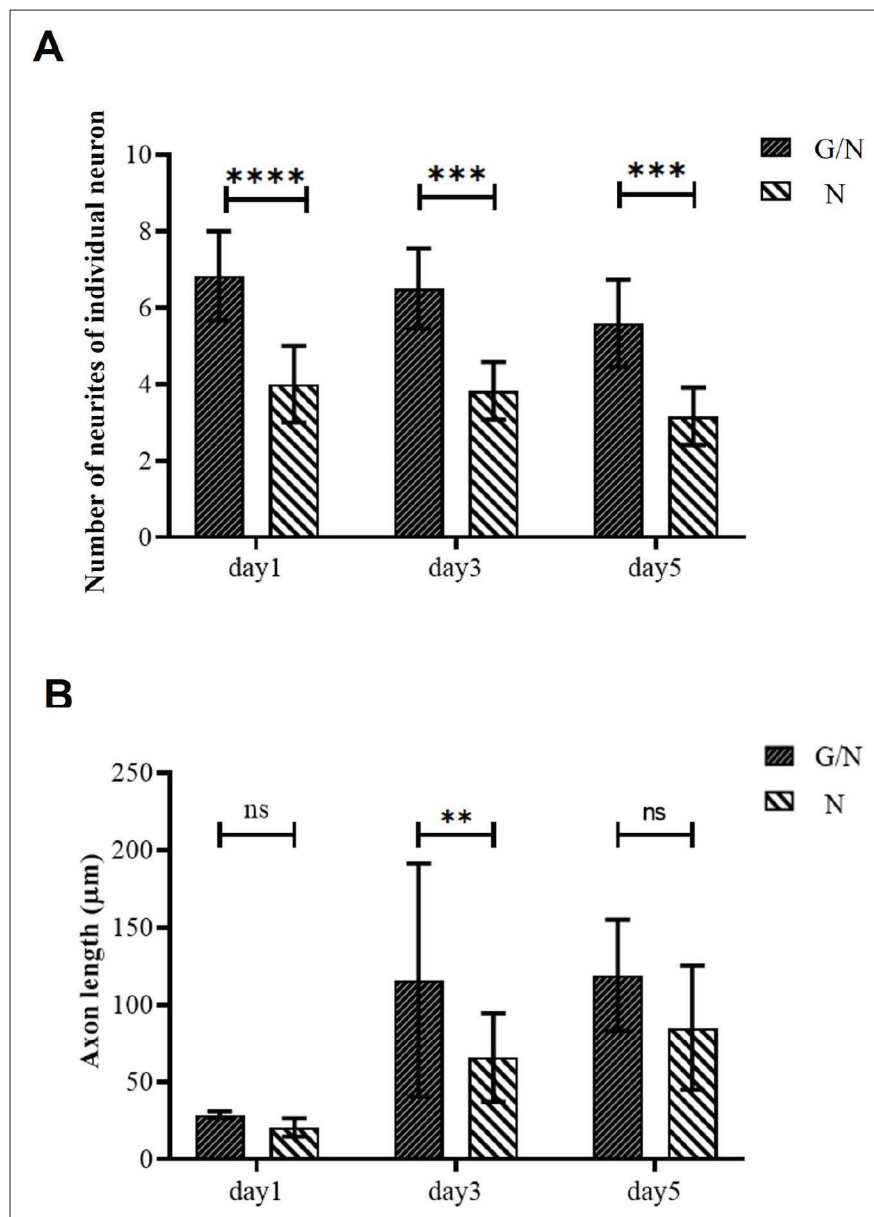
Figure 7. Neurite characteristics of individual neurons in G/N and N after 1, 3, and 5 days of culture. (A) Number of neurites of individual neuron in G/N and N. (B) Axon length of individual neuron in G/N and N. Significance was calculated using two-way ANOVA followed by *t*-test. All error bars are standard deviation. $*p < 0.05$, $**p < 0.01$, $***p < 0.001$, and $****p < 0.0001$, respectively.

method of seeding the mixed cells onto 2D planar cell culture dishes or 3D scaffolds, this method can realize the fabrication of a spatially partitioned co-culture model of neurons and glioma cells, which can best mimic the spatial relationship of neurons and glioma cells in actual glioma tissues. The bioprinted glioma *in vitro* 3D model has a complete and clear demarcation line between neurons area and glioma cells area, which provides an adequate model of glioma tissue.

The microenvironment in which glioma cells live in natural human tissues is complex, and interactions between glioma cells and neurons have important influences for progression of glioma. In the bioprinted glioma *in vitro* 3D model, the glioma cells close to neurons were found elongated with filopodium in morphology. Filopodium is a typical feature of neural cells, and this result indicates that neurons promote the transformation to neuron-like cells of GL261 cells, which is consistent with the phenomenon observed *in vivo*[18] and *in vitro*[16,33,34]. In actual glioma tissues, glioma cells outgrow filopodium to establish electrical connection with neurons around them[18] to enhance invasiveness. But on the other hand,

transformation to neuron-like cells may reduce the proliferative capacity of glioma cells to significantly inhibit tumor growth[35], and prolong the survival time of patients[36]. Thus, the effects of neurons on glioma cells are complex and should be further explored by *in vivo* and *in vitro* experiments.

Neurons cultured in the bioprinted glioma *in vitro* 3D model showed a higher survival rate, more neurites and longer axons. After 1 day of culture, the reason for the low survival rate of neurons in both models may be attributed to the fact that neurons may be damaged in the process of isolation and did not adapt to the 3D matrix materials in the initial stage. After 3 days of culture, with the adaptation of neurons to 3D culture environment, the survival rate of neurons in both models increased significantly (27.36% in G/N and 17.47% in N), and the neurons showed a good spreading and presented a large number of neurites. After 5 days of culture, neurons become apoptotic, resulting in the decline of survival rate[37]. During the 5 days of culturing, the significantly higher survival rate, more neurites and longer axons of neurons in G/N than in G indicates that glioma cells may trigger synaptic differentiation and neuronal process growth[38,39] and increase the hyperexcitability of neural circuits[40-43].

Ca^{2+} is closely related to cell proliferation, neuronal plasticity, and intracellular signal transduction[44-49]. Ca^{2+} can regulate cell behaviors of glioma cells, including cell proliferation, migration, invasion and apoptosis[50-54]. Our results indicated that neurons may promote the expression of Ca^{2+} in glioma cells, which is possibly related to the extracellular K^+ during neuronal activity[17], but needs to be verified by further experiments. During the development of glioma, Ca^{2+} activates ERK/MAPKs[55] and PKA[56] pathways of glioma cells and promotes glioma cells to produce synaptic plasticity required for migration and invasion[57], so as to promote glioma progression[44], which may further explain that GL261 cells around neurons in our study have experienced neuron-like transformation and increased in number when their intercellular Ca^{2+} concentration increased. On the other hand, the increase of Ca^{2+} in glioma cells may stimulate glioma cells to produce glutamate and release it to surrounding cells[58-60], leading to the excitotoxicity and the enhancement of synaptic plasticity of surrounding neurons, which can further explain that neurons near GL261 cells in our study show more neurites and longer axons. In addition, the increase of glutamate caused by the increase of Ca^{2+} can further stimulate the growth of adjacent glioma cells[61,62]. All these evidences, combined with our results, indicate that one of the ways that neurons promote glioma progression is to promote the expression of Ca^{2+} in glioma cells[63], leading to the deterioration of glioma[64]. Therefore, targeting

Ca^{2+} signaling pathway may be a new strategy for glioma treatment[65].

Our results support the idea that the interactions between neurons and glioma cells are complex and bidirectional[37]. Ideally, new antiglioma therapies should take advantages of the cell–cell interactions in glioma tissues to minimize the damage and improve the efficacy[66]. For example, in clinical and research settings, noninvasive brain stimulation (NiBS) involves applying magnetic or electrical fields to modify neuronal activity[67] in order to modulate the behaviors of glioma cells, so as to influence the development of glioma. However, the mechanism of this treatment is still unclear and its efficacy is difficult to predict. The studies about the complex interactions between glioma cells and their surrounding neurons are urgently needed to improve the understanding and therapies. Herein, the bioprinted glioma *in vitro* 3D model provides a novel model to understand and utilize the complex interactions between glioma cells and their surrounding neurons, and a two-way promotion relationship between glioma cells and neurons around them in the early stage of glioma is shown, which will promote the development of new glioma treatment methods, such as NiBS.

The complex microenvironment of glioma includes multiple cells and biochemical factors, which matters in the progression of glioma[5]. In this study, we only included neurons and glioma cells, which results in an inconspicuous glioma invasion. Besides, cells like astrocytes and microglia support the survival and function of neurons[68], and the lack of these cells leads to the imbalance of the microenvironment of the model; therefore, the survival time of the model is short and then, the neuron death occurs. However, since 3D printing can produce complex structures containing multiple materials, it is promising to integrate other cells and biochemical factors in this model to make it closer to natural glioma tissue to solve existing problems and provide more accurate pathological and pharmacological models for glioma in the future.

5. Conclusion

In this study, a bioprinted glioma *in vitro* 3D model was constructed using a step-by-step bioprinting method to reproducibly and better control the spatial relationship between glioma cells and neurons in natural human glioma tissue. Our findings indicated that the proposed bioprinted glioma *in vitro* 3D model is better suited to mimic the state of glioma encapsulated by neurons found *in vivo*. In the bioprinted glioma *in vitro* 3D model, the glioma cells around neurons showed larger number, neuron-like morphology, and higher intracellular Ca^{2+} concentration. An appropriate amount of glioma cells was found to

improve the survival rate of neurons and synaptic growth in the bioprinted glioma *in vitro* 3D model. These results are an indication of the two-way promotion relationship between glioma cells and neurons around them in the early stage of glioma. A better understanding of this under-recognized phenomenon that occurs in the glioma tissue may reveal promising new approaches for the development of novel therapeutics and personalized treatments aimed at addressing such devastating group of neural cancers. Besides, this study proves that reproducing the *in vivo* events in 3D-printed glioma model is possible, which is promising in promoting personalized 3D pharmacological and pathological glioma model.

Acknowledgments

None.

Funding

Conflict of interest

The authors declare no conflict of interests.

Author contributions

Conceptualization: Ling Wang, Xinggang Mao, Na Pei, Luge Bai
Formal analysis: Luge Bai, Na Pei
Funding acquisition: Luge Bai, Zhiyan Hao, Sen Wang, Jiajia Zhou, Siqi Yao
Investigation: Luge Bai, Na Pei
Methodology: Luge Bai, Na Pei, Xinggang Mao, Ling Wang
Resources: Sen Wang, Jiajia Zhou, Na Pei, Kun Zhang
Supervision: Jiankang He, Dichen Li
Writing – original draft: Luge Bai
Writing – review & editing: Hui Zhu, Kun Zhang, J. Miguel Oliveira, Rui L. Reis, Xinggang Mao, Ling Wang

Ethics approval and consent to participate

All animal experiments were approved and performed in accordance with the protocols approved by the Animal Ethics Committee at Xi'an Jiaotong University (protocol code 2022-15 and date of approval is March 1, 2022).

Consent for publication

Not applicable.

Availability of data

Not applicable.

References

1. Li Z, Li M, Xia P, *et al.*, 2022, Targeting long non-coding RNA PVT1/TGF-β/Smad by p53 prevents glioma progression. *Cancer Biol Ther*, 23(1):225–233.

2. Weller M, Cloughesy T, Perry JR, *et al.*, 2013, Standards of care for treatment of recurrent glioblastoma—Are we there yet? *Neuro-Oncology*, 15(1):4–27.

3. Bobustuc GC, Baker CH, Limaye A, *et al.*, 2010, Levetiracetam enhances p53-mediated MGMT inhibition and sensitizes glioblastoma cells to temozolomide. *Neuro-Oncology*, 12(9):917–927.

4. Chen Y, Henson ES, Xiao W, *et al.*, 2016, Bcl-2 family member Mcl-1 expression is reduced under hypoxia by the E3 ligase FBW7 contributing to BNIP3 induced cell death in glioma cells. *Cancer Biol Ther*, 17(6):604–613.

5. Wang C, Tong X, Yang F, 2014, Bioengineered 3D brain tumor model to elucidate the effects of matrix stiffness on glioblastoma cell behavior using PEG-based hydrogels. *Mol Pharm*, 11(7):2115–2125.

6. Xu X, Li L, Luo L, *et al.*, 2021, Opportunities and challenges of glioma organoids. *Cell Commun Signal,* 19(1):1–13.

7. Zhang C, Jin M, Zhao J, *et al.*, 2020, Organoid models of glioblastoma: Advances, applications and challenges. *Am J Cancer Res*, 10(8):2242–2257.

8. De Witt Hamer PC, Van Tilborg AAG, Eijk PP, *et al.*, 2008, The genomic profile of human malignant glioma is altered early in primary cell culture and preserved in spheroids. *Oncogene*, 27(14):2091–2096.

9. Wang X, Prager BC, Wu Q, *et al.*, 2018, Reciprocal signaling between glioblastoma stem cells and differentiated tumor cells promotes malignant progression. *Cell Stem Cell*, 22(4):514–528.

10. Goers L, Freemont P, Polizzi KM, 2014, Co-culture systems and technologies: Taking synthetic biology to the next level. *J R Soc Interface*, 11(96):20140065.

11. Singh SK, Hawkins C, Clarke ID, *et al.*, 2004, Identification of human brain tumour initiating cells. *Nature*, 432(7015): 396–401.

12. Yuan X, Curtin J, Xiong Y, *et al.*, 2004, Isolation of cancer stem cells from adult glioblastoma multiforme. *Oncogene*, 23(58):9392–9400.

13. Mirab F, Kang YJ, Majd S, 2019, Preparation and characterization of size-controlled glioma spheroids using agarose hydrogel microwells. *PLoS One*, 14(1):e0211078.

14. Barresi V, Belluardo N, Sipione S, *et al.*, 2003, Transplantation of prodrug-converting neural progenitor cells for brain tumor therapy. *Cancer Gene Ther*, 10(5):396–402.

15. Liu Y, Carlsson R, Ambjørn M, *et al.*, 2013, PD-L1 expression by neurons nearby tumors indicates better prognosis in glioblastoma patients. *J Neurosci*, 33(35):14231–14245.

16. Gillespie S, Monje M, 2018, An active role for neurons in glioma progression: Making sense of Scherer's structures. *Neuro-Oncology*, 20(10):1292–1299.

17. Scherer HJ, 1938, Structural development in gliomas. *Am J Cancer*, 34(3):333–351.

18. Venkatesh HS, Morishita W, Geraghty AC, *et al.*, 2019, Electrical and synaptic integration of glioma into neural circuits. *Nature*, 573(7775):539–545.

19. Fu YS, Lin YY, Chou SC, *et al.*, 2008, Tetramethylpyrazine inhibits activities of glioma cells and glutamate neuro-excitotoxicity: Potential therapeutic application for treatment of gliomas. *Neuro-Oncology*, 10(2):139–152.

20. Chaunsali L, Tewari BP, Gallucci A, *et al.*, 2020, Glioma-induced peritumoral hyperexcitability in a pediatric glioma model. *Physiol Rep*, 8(19):e14567.

21. Wei Z, Kale S, El Fatimy R, *et al.*, 2019, Co-cultures of glioma stem cells and primary neurons, astrocytes, microglia, and endothelial cells for investigation of intercellular communication in the brain. *Front Neurosci-Switz*, 13:361.

22. Fuchs Q, Batut A, Gleyzes M, *et al.*, 2021, Co-culture of glutamatergic neurons and pediatric high-grade glioma cells into microfluidic devices to assess electrical interactions. *JoVE*, 16(177):e62748.

23. Saunders RE, Derby B, 2014, Inkjet printing biomaterials for tissue engineering: Bioprinting. *Int Mater Rev*, 59(8): 430–448.

24. Schiele NR, Corr DT, Huang Y, *et al.*, 2010, Laser-based direct-write techniques for cell printing. *Biofabrication*, 2(3):032001.

25. Gu Z, Fu J, Lin H, *et al.*, 2020, Development of 3D bioprinting: From printing methods to biomedical applications. *Asian J Pharm Sci*, 15(5):529–557.

26. Ji S, Guvendiren M, 2021, Complex 3D bioprinting methods. *APL Bioeng*, 5(1):011508.

27. Choudhury D, Tun HW, Wang T, *et al.*, 2018, Organ-derived decellularized extracellular matrix: A game changer for bioink manufacturing? *Trends Biotechnol*, 36(8):787–805.

28. Sorushanova A, Delgado LM, Wu Z, *et al.*, 2019, The collagen suprafamily: From biosynthesis to advanced biomaterial development. *Adv Mater*, 31(1):1801651.

29. Di Nunno V, Franceschi E, Tosoni A, *et al.*, 2022, Tumor-associated microenvironment of adult gliomas: A review. *Front Oncol*, 12:891543.

30. Gómez-Oliva R, Domínguez-García S, Carrascal L, *et al.*, 2021, Evolution of experimental models in the study of glioblastoma: Toward finding efficient treatments. *Front Oncol,* 10:614295.

31. Wang X, Li X, Ding J, *et al.*, 2021, 3D bioprinted glioma microenvironment for glioma vascularization. *J Biomed Mater Res Part A*, 109(6):915–925.

32. Cha J, Kim P, 2017, Biomimetic strategies for the glioblastoma microenvironment. *Front Mater,* 4:45.

33. Zhao J, He H, Zhou K, *et al.*, 2012, Neuronal transcription factors induce conversion of human glioma cells to neurons and inhibit tumorigenesis. *PLoS One*, 7(7):41506–41517.

34. Su Z, Zang T, Liu ML, *et al.*, 2014, Reprogramming the fate of human glioma cells to impede brain tumor development. *Cell Death Discov,* 5(10):e1463–e1463.

35. Fu JQ, Chen Z, Hu YJ, *et al.*, 2019, A single factor induces neuronal differentiation to suppress glioma cell growth. *CNS Neurosci Ther*, 25(4):486–495.

36. Yan T, Skaftnesmo KO, Leiss L, *et al.*, 2011, Neuronal markers are expressed in human gliomas and NSE knockdown sensitizes glioblastoma cells to radiotherapy and temozolomide. *BMC Cancer*, 11(1):1–11.

37. Li F, Zhang W, Wang M, *et al.*, 2020, IL1RAP regulated by PRPRD promotes gliomas progression via inducing neuronal synapse development and neuron differentiation in vitro. *Pathol Res Pract*, 216(11):153141.

38. Nagaraja S, Vitanza NA, Woo PJ, *et al.*, 2017, Transcriptional dependencies in diffuse intrinsic pontine glioma. *Cancer Cell*, 31(5):635–652.

39. Lawn S, Krishna N, Pisklakova A, *et al.*, 2015, Neurotrophin signaling via TrkB and TrkC receptors promotes the growth of brain tumor-initiating cells. *J Biol Chem*, 290(6):3814–3824.

40. Aryal M, Vykhodtseva N, Zhang YZ, *et al.*, 2013, Multiple treatments with liposomal doxorubicin and ultrasound-induced disruption of blood–tumor and blood–brain barriers improve outcomes in a rat glioma model. *J Controlled Release*, 169(1–2):103–111.

41. Buckingham SC, Campbell SL, Haas BR, *et al.*, 2011, Glutamate release by primary brain tumors induces epileptic activity. *Nat Med*, 17(10):1269–1274.

42. Campbell SL, Buckingham SC, Sontheimer H, 2012, Human glioma cells induce hyperexcitability in cortical networks. *Epilepsia*, 53(8):1360–1370.

43. Johung T, Monje M, 2017, Neuronal activity in the glioma microenvironment. *Curr Opin Neurobiol*, 47:156–161.

44. Pei Z, Lee KC, Khan A, *et al.*, 2020, Pathway analysis of glutamate-mediated, calcium-related signaling in glioma progression. *Biochem Pharmacol*, 176:113814.

45. Leclerc C, Haeich J, Aulestia FJ, *et al.*, 2016, Calcium signaling orchestrates glioblastoma development: Facts and conjunctures. *Biochim Biophys Acta Mol Cell Res*, 1863(6):1447–1459.

46. Zündorf G, Reiser G, 2011, Calcium dysregulation and homeostasis of neural calcium in the molecular mechanisms

of neurodegenerative diseases provide multiple targets for neuroprotection. *Antioxid Redox Signal,* 14(7):1275–1288.

47. Prevarskaya N, Skryma R, Shuba Y, 2011, Calcium in tumour metastasis: New roles for known actors. *Nat Rev Cancer*, 11(8):609–618.

48. Marchi S, Pinton P, 2016, Alterations of calcium homeostasis in cancer cells. *Curr Opin Pharmacol*, 29:1–6.

49. Déliot N, Constantin B, 2015, Plasma membrane calcium channels in cancer: Alterations and consequences for cell proliferation and migration. *Biochim Biophys Acta Biomembr*, 1848(10):2512–2522.

50. Lang F, Stournaras C, 2014, Ion channels in cancer: future perspectives and clinical potential. *Philos Trans R Soc B*, 369(1638):20130108.

51. Chen WL, Turlova E, Sun CLF, *et al.*, 2015, Xyloketal B suppresses glioblastoma cell proliferation and migration in vitro through inhibiting TRPM7-regulated PI3K/Akt and MEK/ERK signaling pathways. *Mar Drugs*, 13(4): 2505–2525.

52. Morrone FB, Gehring MP, Nicoletti NF, 2016, Calcium channels and associated receptors in malignant brain tumor therapy. *Mol Pharmacol*, 90(3):403–409.

53. Wee S, Niklasson M, Marinescu VD, *et al.*, 2014, Selective calcium sensitivity in immature glioma cancer stem cells. *PLoS One*, 9(12):e115698.

54. Berridge MJ, Bootman MD, Roderick HL, 2003, Calcium signalling: Dynamics, homeostasis and remodelling. *Nat Rev Mol Cell Biol*, 4(7):517–529.

55. Wiegert JS, Bading H, 2011, Activity-dependent calcium signaling and ERK-MAP kinases in neurons: A link to structural plasticity of the nucleus and gene transcription regulation. *Cell Calcium*, 49(5):296–305.

56. Danbolt NC, 2001, Glutamate uptake. *Prog Neurobiol*, 65(1):1–105.

57. Barria A, 2019, Dangerous liaisons as tumour cells form synapses with neurons. *Nature*, 573:499–501.

58. Parpura V, Grubišić V, Verkhratsky A, 2011, Ca2+ sources for the exocytotic release of glutamate from astrocytes. *Biochim Biophys Acta Mol Cell Res*, 1813(5):984–991.

59. Malarkey EB, Parpura V, 2008, Mechanisms of glutamate release from astrocytes. *Neurochem Int*, 52(1–2):142–154.

60. Metea MR, Newman EA, 2006, Calcium signaling in specialized glial cells. *Glia*, 54(7):650–655.

61. Ye ZC, Sontheimer H, 1999, Glioma cells release excitotoxic concentrations of glutamate. *Cancer Res*, 59(17):4383–4391.

62. Sontheimer H, 2008, A role for glutamate in growth and invasion of primary brain tumors. *J Neurochem*, 105(2): 287–295.

63. Maklad A, Sharma A, Azimi I, 2019, Calcium signaling in brain cancers: Roles and therapeutic targeting. *Cancers*, 11(2):145.

64. Wypych D, Pomorski P, 2013, Calcium signaling in glioma cells—The role of nucleotide receptors. *Glioma Signal*, 986:61–79.

65. Lin C, Chen J, Su Z, *et al.*, 2021, A calcium-related immune signature in prognosis prediction of patients with glioma. *Front Cell Dev Biol*, 9:2740.

66. Vannini E, Olimpico F, Middei S, *et al.*, 2016, Electrophysiology of glioma: A Rho GTPase-activating protein reduces tumor growth and spares neuron structure and function. *Neuro Oncol*, 18(12):1634–1643.

67. Sprugnoli G, Golby AJ, Santarnecchi E, 2021, Newly discovered neuron-to-glioma communication: New noninvasive therapeutic opportunities on the horizon? *Neurooncol Adv*, 3(1):vdab018.

68. Zhang Y, Sloan SA, Clarke LE, *et al.*, 2016, Purification and characterization of progenitor and mature human astrocytes reveals transcriptional and functional differences with mouse. *Neuron*, 89(1):37–53.